Enhanced Photovoltaic Performance of Dye-Sensitized Solar Cells Using TiO_2-Graphene Microplatelets Hybrid Photoanode

Umer Mehmood, Khalil Harrabi, Ibnelwaleed A. Hussein, and Shakeel Ahmed

***Abstract*—Hybrid photoanodes for dye-sensitized solar cells (DSSCs) were prepared by simple addition of graphene (GR) microplatelets to TiO_2 nanoparticulate paste. Transmission electron microscopy was used to confirm the presence of GR in composite films after heating at 450 °C for 30 min. TiO_2/GR-based DSSCs were fabricated using an N749 photosensitizer. The UV–Visible absorption spectroscopy, photocurrent–voltage (*I–V*) characteristic, and electrochemical impedance spectroscopy measurements were carried out to characterize the cells. The results indicate that the GR/TiO_2 photoanode improves the performance of the solar cell. This is because the GR/titania electrode accelerates electronic transportation and suppresses the charge recombination. Under optimal conditions, the solar cell based on GR/TiO_2 shows power conversion efficiency (PCE) of 4.1%, which is about 30% greater than the cell based on the pristine TiO_2 electrode (3.16%). The objective of this study is to develop a fast, cheap, and an effective means to increase the PCE of DSSCs. Density functional theory was used to calculate the bandgap of TiO_2 and graphnene-TiO_2.**

***Index Terms*—Dye-sensitized solar cell (DSSC), graphene (GR), nanocomposite photoanodes, power conversion efficiency (PCE), titania.**

I. Introduction

THE increasingly serious energy crisis and the environmental contamination caused by the burning of fossil fuels have led to an aggressive search for renewable and environmental-friendly energy resources. The use of renewable energy provides benefits that reduce emissions of air pollutants, as well as greenhouse gases. Therefore, alternative sources of energy are needed so that mankind can survive on the Earth without depending on fossil fuels. Solar energy is one of the renewable energy sources that will contribute to the security of future energy supplies [1], [2]. Solar radiation from the sun is approximately 310^{24} J per year, which is ten times the current energy demand [3]. Light from the sun can be harvested by dye-sensitized solar cells (DSSCs). DSSCs have attracted considerable attention during the last decade due to an ideal compromise between efficiency and cost performance [4]–[6]. DSSCs comprise of a sensitized semiconductor (photoelectrode) and a catalytic electrode (counter electrode) with an electrolyte sandwiched between them. The key component of the DSSCs is a dye. Its function is to absorb incoming sunlight and produce excitons. It is chemically bonded to the porous surface of a metal oxide semiconductor. So far, polypyridyl ruthenium sensitizer-based solar cells have attained up to 11% conversion efficiency [7]–[9]. However, it is still low for commercial applications.

The major cause of the low efficiency of DSSCs is the recombination of injected electrons (from the dye to the conduction band of the semiconductor) with the electrolyte (dark current) [10], [11]. The photoanode of DSSCs plays an important role in the separation and transportation of electrons. Carbon-based materials (CNTs) [12], [13] and, more recently, graphene (GR) [14], [15] have been proposed as an additive material for TiO_2 photoanode to increase the electron mobility, owing to their outstanding electronic properties. However, the enhancement of power conversion efficiency (PCE) due to CNTs is limited by poor contact between CNTs and TiO_2 [16]. Two-dimensional GR nanocarbon materials were also introduced to prepare the hybrid film [17]. It has an excellent mobility of charge carrier (200 000 $cm^2 \cdot V^{-1} \cdot s^{-1}$) [18] and large specific surface area (2630 m^2/g) [19]. Mehmood *et al.* [17] introduced GR into TiO_2 by one-step hydrothermal reaction and reported a 17.7% increase in PCE of DSSC. Tang *et al.* [20] embedded GR sheets in TiO_2 paste via molecular grafting and showed 1.68% efficiency, which is five times higher than that without GR (0.32%). Sun *et al.* [21] fabricated GR/TiO_2 nanocomposites electrode through the heterogeneous coagulation method and reported 4.28% efficiency, which is 59% greater than that without GR. However, the efficiency of these cells is still lower, and the fabrication methods of graphing/TiO_2 nanocomposite are relatively complex. Here, we presented a fast, cheap, and one-step process to prepare the GR/TiO_2 photoanode. It is expected that the incorporation of GR in the photanode may enhance the PCE of DSSCs by reducing the charge recombination.

Manuscript received July 1, 2015; revised August 31, 2015; accepted September 14, 2015. Date of publication September 30, 2015; date of current version December 18, 2015. This work was supported by the King Abdulaziz City for Science and Technology (KACST) through the Science and Technology Unit, King Fahd University of Petroleum and Minerals, through Project # 11-ENE1635-04 as part of the National Science, Technology, and Innovation Plan.

U. Mehmood is with the Department of Chemical Engineering, King Fahd University of Petroleum and Minerals, Dhahran 31261, Saudi Arabia, and also with the Polymer and Process Engineering Department, University of Engineering and Technology, Lahore, Pakistan (e-mail: umermehmood@kfupm.edu.sa).

K. Harrabi is with the Department of Physics, King Fahd University of Petroleum and Minerals, Dhahran 31261, Saudi Arabia (e-mail: harrabi@kfupm.edu.sa).

I. A. Hussein is with the Department of Chemical Engineering, King Fahd University of Petroleum and Minerals, Dhahran 31261, Saudi Arabia, and also with the Gas Processing Center, College of Engineering, Qatar University, Doha, Qatar (e-mail: ihussein@kfupm.edu.sa).

S. Ahmed is with Department of Chemistry, King Fahd University of Petroleum and Minerals, Dhahran 31261, Saudi Arabia (e-mail: shakeel@kfupm.edu.sa).

Color versions of one or more of the figures in this paper are available online at http://ieeexplore.ieee.org.

Digital Object Identifier 10.1109/JPHOTOV.2015.2479468

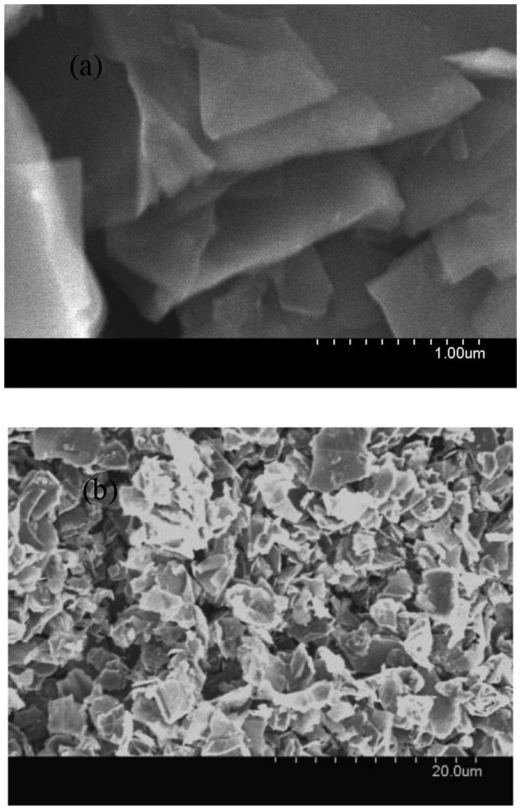

Fig. 1. SEM images of GR sheets at different magnification. (a) 1 μm and (b) 20 μm.

II. Computer Simulation

All the DFT calculations were executed using Amsterdam Density Functional program (2013.01). BAND mode was used to simulate the anatase TiO_2 clusters. The tetragonal anatase crystal structure was selected with single layer (0 0 1) surface slab. Then, we created 2×2 super cell from this slab [22]. All atoms were mapped within the unit cell. GR is an allotrope of carbon in the form of a 2-D sheet. TiO_2- and GR-doped TiO_2 models were simulated by considering hybrid Becke parameter, Lee–Yang–Parr (B1YLP) level, and triple-ζ polarization basis function. In all the calculations, the relativistic effects were taken into account by the zero-order regular approximation Hamiltonian in its scalar approximation [23], [24].

III. Experimental Details

A. Preparation of Composite Anodes

Fig. 1 shows the scanning electron microscope (SEM) images of GR. It clearly shows the different layers of GR. The specifications of GR are shown in Table I. A suspension of ethanol and GR was prepared by dissolving 15 mg of GR (purchased from Grafen Chemical Industries Co., Turkey) in 20-ml ethanol. It was then sonicated for 5 h to attain a good dispersion of GR in ethanol. An exact quantity of dispersed GR was mixed with known amount of anatase TiO_2 paste (T/SP 14451, Solaronix) to obtain a composite paste. Five different samples of TiO_2-GR were prepared by varying the composition of GRs, i.e., 0, 0.03, 0.06, 0.09, 0.12, and 0.15 wt%. The composite paste was then tape casted on fluorine-doped tin oxide (FTO) glass substrate (2 mm, 7 Ω/seq, Solaronix). The coated glass substrate annealed at 450 °C for 30 min. Other photoanodes were prepared following the same procedure. The thickness of each photoanode was found by using cross-sectional images obtained from SEM (JEOL, 6610LV). The average thickness of each film was 8 μm.

TABLE I
Specifications of GR

Property	Values
Specific surface area	100 m^2/g
Purity	99.9%
Average flake thickness	8 nm (20–30 monolayers)
Average Particle (lateral) size	(150–3000) nm

B. Fabrication of Dye-Sensitized Solar Cells

A 0.5-mM solution of N749 was prepared in methanol. The composite electrodes were soaked in the dye solution for 24 h. After sensitization, the samples were washed with ethanol to eliminate unanchored dye. Then, DSSCs were fabricated by employing the sensitized hybrid anode, platinum-deposited counter electrode (Plasticol T, Solaronix), 60-μm sealing spacer (Meltonix 1170, Solaronix), and I^-/I_3^- redox couple electrolyte prepared in methoxypropionitrile with a 50-mM redox concentration (Iodolyte Z-50, Solaronix).

C. Characterization of Dye-Sensitized Solar Cells

The visible spectra of N719 in methanol and adsorbed on TiO_2 films at glass substrates were recorded with a JASCO-670 UV/VIS spectrophotometer. A Keithley 2400 Source Meter was used to measure the *I–V* characteristics of the DSSCs using IV-5 solar simulator (Sr #83, PV Measurement, Inc.) at AM1.5G (100 $mW \cdot cm^{-2}$). The silicon solar cell was used as a reference for calibration. The electrochemical impedance spectroscopy (EIS) was measured in dark conditions of illumination via Bio-Logic SAS (VMP3, s/n: 0373), with an ac signal of 10 mV in amplitude, in the frequency range between 10 mHz and 1 MHz.

IV. Results and Discussion

The dispersion of GR in TiO_2 was observed by transmission electron microscopy (TEM) (JEOL, JEM-2100F) analysis. TiO_2- GR sample having 0.15% GR was selected for TEM analysis, because it was difficult to obtain TEM images of dispersed GR in TiO_2 from low-concentration samples. Fig. 2(a) shows the TEM image of titania. Fig. 2(b) clearly demonstrates the crystalline nature of the GR sheet. High-resolution TEM was used to measure the GR layer spacing in its crystalline lattice. The lattice spacing in GR prepared by our method is 0.348 nm. Fig. 2(c) shows the nanocomposite of GR-TiO_2. Fig. 2(c) also shows that GR nanosheets tend to congregate together to form multilayer agglomerates.

The highest occupied molecular orbitals (HOMOs), lowest unoccupied molecular orbitals (LUMOs), and bandgap energies

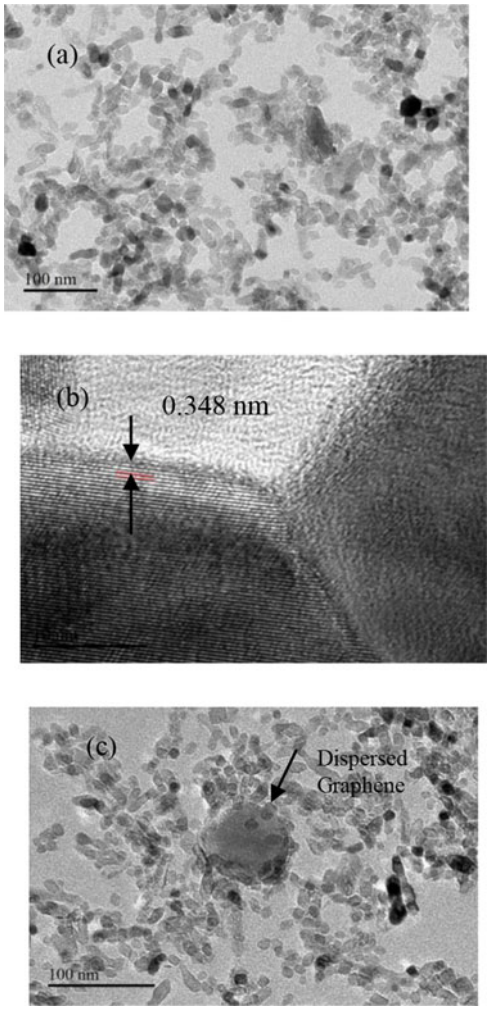

Fig. 2. TEM images of (a) TiO_2 nanoparticles, (b) lattice spacing in GR, and (c) TiO_2-GR nanocomposites.

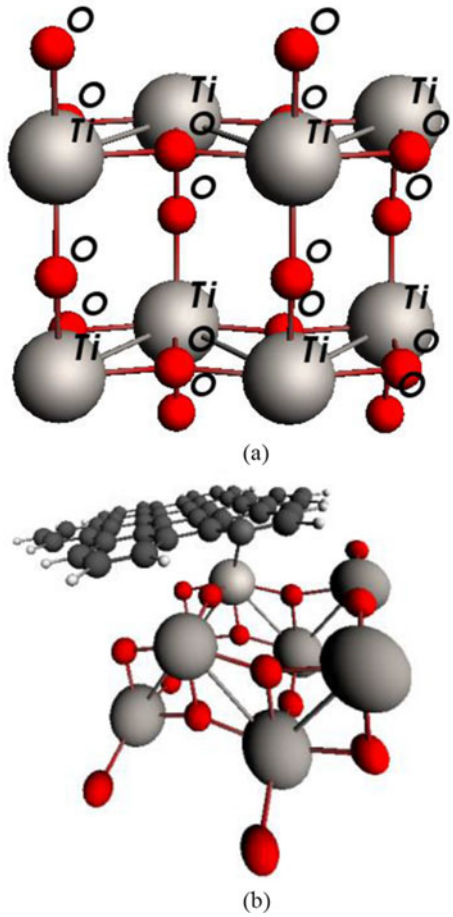

Fig. 3. Simulated structures of (a) TiO_2 and (b) GR-doped TiO_2.

TABLE II
SIMULATED ELECTRONIC STRUCTURE PROPERTIES OF TiO_2 AND GR-DOPED TiO_2

System	E_{CB} (eV)	V_B (eV)	Bandgap (eV)
TiO_2	–4.10	–7.20	3.1
GR-TiO_2	–4.30	–6.80	2.5

of photosensitizers play a vital role in providing the driving force for the electron injection to conduction band of TiO_2. For efficient charge transfer, the LUMOs of dyes must be more negative than the conduction band of the semiconductor, while HOMO levels must be more positive than the redox potential of electrolyte. We used a DFT technique to find the bandgap of TiO_2 and GR-TiO_2. The simulated structures of TiO_2 and GR-TiO_2 are shown in Fig. 3, while the simulated conduction band, valence band, and bandgap of TiO_2 and GR-TiO_2 are shown in Table II. These results are in good agreement with the experimental values [25]–[27]. The computed results show that impregnation of GR reduces the bandgap of TiO_2. This is because the GR possesses the lower value of the E_{CB} ($\sim$0 EV versus NHE) [28] than that of the titania (-0.5 eV versus NHE) [29]. The charge equilibrium between GR and TiO_2 would cause a shift of apparent Fermi level (E_F) to more positive potential. Moreover, the downward positive shift due to GR can cause a significant driving force to expedite the electron transport from the sensitizer to the photoanode.

The visible spectra of N749 in methanol and anchored to TiO_2 and TiO_2-GR are shown in Fig. 4(a) and (b), respectively. The two broad visible bands at 608 and 415 nm in N749 are assigned to the metal-to-ligand charge-transfer origin. The bands in the UV at 322 nm are assigned as intraligand (π–π^*) charge-transfer transitions. However, the absorption shifts to lower energy values when anchored to TiO_2 and TiO_2-GR. This is due to the fact that on the electrode, the carboxylate groups bind to the TiO_2 surface in which Ti^{4+} acts as proton. The interaction between the carboxylate group and the surface Ti^{4+} ions may lead to increased delocalization of the π^* orbital. The energy of the π^* level is decreased by this delocalization, which explains the red shift for the absorption spectra. However, the TiO_2-GR-based photoanode has a greater red shift value as compared with pure TiO_2. This is because the GR may exhibit photosensitizing properties, thus extending photovoltaic properties into the visible spectrum [30], [31].

Hybrid GR/TiO_2-based DSSCs were prepared with an effective area of 0.35 cm^2. The photovoltaic parameters such as

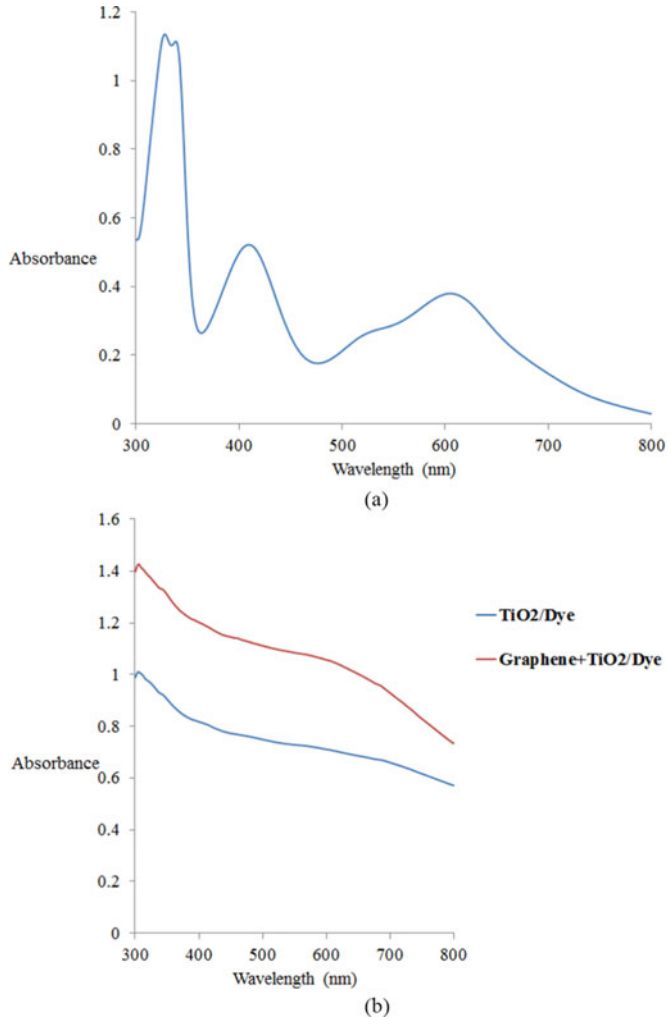

Fig. 4. (a). UV–Vis spectra of N749 in methanol. (b). UV–Vis spectra of TiO_2/N749 and 0.09%GR+TiO_2/N749.

TABLE III
PHOTOVOLTAIC PROPERTIES OF DSSCS

DSSCs	j_{sc} (mA/cm^2)	V_{oc} (mV)	FF(%)	η (%)	R_{sh} (Ω)	R_s (Ω)
Pure TiO_2	10.310	703.994	43.50	3.16	1090	239
0.03%GR+TiO_2	12.089	705.088	42.31	3.61	803	204
0.06%GR+TiO_2	14.181	706.786	38.84	3.89	528	159
0.09%GR+TiO_2	13.037	705.022	43.90	4.03	1453	196
0.12%GR+TiO_2	12.195	696.490	40.02	3.40	1353	189
0.15%GR+TiO_2	9.1850	690.836	47.52	3.02	2390	294

short-circuit current density (J_{sc}), open-circuit voltage (V_{oc}), fill factor (FF), photovoltaic conversion efficiency (η), shunt resistances (R_{sh}), and series resistances (R_s) are summarized in Table III, and the corresponding *I–V* curves are shown in Fig. 5. The DSSC with the highest efficiency is achieved in the case of 0.09% GR-TiO_2, which is about 30% greater than the unmodified TiO_2 (3.16).

This is because of the improved charge collection at composite photoanode. The addition of a small amount of GR to the TiO_2 anode is claimed to create a 3-D percolating network of

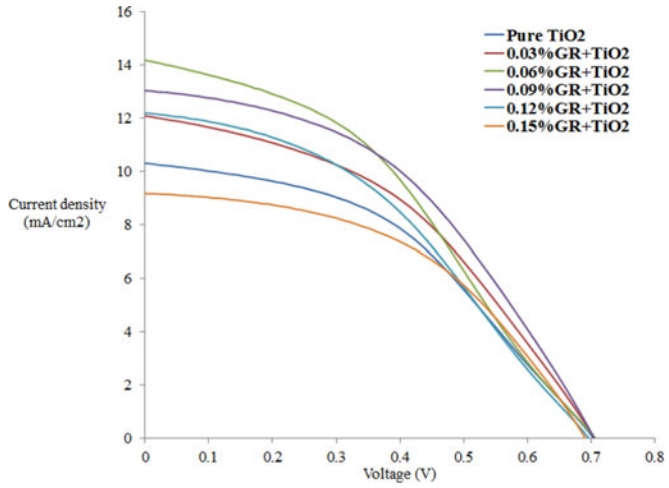

Fig. 5. Current–voltage characteristics of DSSCs fabricated using different contents of GR.

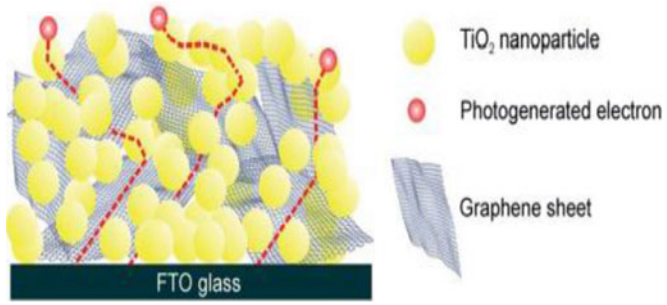

Fig. 6. Concept of improved charge collection in a photoanode based on a 3-D GR network embedded in a TiO_2 mesoporous structure [11].

a highly conducting and almost transparent material perfectly matching the electron band alignment between the TiO_2 and the FTO conducting glass (as shown in Fig. 6), offering an efficient pathway for fast collection of photogenerated electrons. However, the little decline in V_{oc} at increasing GR contents could be attributed to the downshift of the potential band edge of the TiO_2 conduction band. It can also be observed that an increase in GR concentration from optimum level (0.09%) negatively affects the performance of DSSCs. This is because of the decrease in film transparency owing to the increase in GR contents. Another possibility of low efficiency at high-GR contents could be attributed to the formation of GR agglomerates inside the TiO_2 matrix acting as trapping sites that obstruct the fast charge collection at the electrodes. The less charge collection together with light loss owing to GR direct absorption strongly declines the efficiency of DSSCs at high-GR contents. Moreover, low FF is another cause of low efficiency of DSSCs. As FF depends on both R_s (should be low) and R_{sh} (should be high), the FF values are low for these DSSCs (see Table II), which is supported by the measured high R_s and low R_{sh} values (see Table III). The low shunt resistance causes power losses in solar cells by providing an alternate pathway for the light-generated current, which lowers FF. R_{sh} should be of the order of 10^3 Ω for a highly efficient solar cell [13]. The high series resistance (R_s) is mainly due to large thickness of the platinum counter electrode

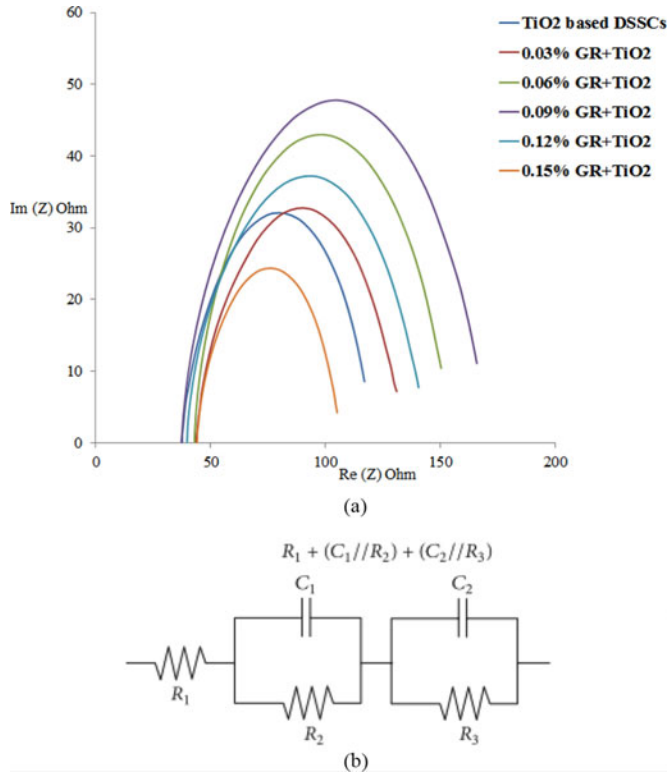

Fig. 7. EIS investigation of TiO_2 and GR+TiO_2-based DSSCs. (b) Equivalent circuit model of the DSSCs.

or the electrolyte layer [32], while low shunt resistance $(R_{\rm sh})$ can be attributed to an inefficient fabrication process of DSSCs [33].

EIS analysis is performed to further explain the photovoltaic properties of DSSCs. Fig. 7 shows the Nyquist plots and the equivalent circuit of DSSCs, which were assembled with TiO_2-N749 and GR-TiO_2-N749. Generally, a normal impedance spectrum of DSSCs is represented by three arcs (semicircles). The first semicircle represents the charge transport resistance at counter electrode/electrolyte (R_1), second signifies the charge transport resistance at the photoanode/electrolyte interface (R_2), and the third indicates the diffusion process of redox couple in electrolyte (*Zw)* [29], [34]. Only the second arc comes out in the Nyquist plot in Fig 5. It is probable that the other two arcs corresponding to R_1 and *Zw* are overshadowed by larger semicircle reprinting R_2 [35], [36]. R_2 is related to the charge recombination rate, e.g., a high R_2 value shows a lower charge recombination and *vice versa*. The R_2 value for DSSC assembled with pure TiO_2 is smaller than that of 0.09% GR-TiO_2, proposing charge recombination is greatly reduced owing to the incorporation of GR. However, the GR concentration greater than 0.09 wt% will lead to the smaller values of R_2 due to a shorter electron lifetime on the order of a few tens of milliseconds [37].

V. Conclusion

We have established a fast and highly reproducible methodology to fabricate DSSCs by simple addition of GR sheets into a TiO_2. The incorporation of GR in TiO_2 slows the recombination of photogenerated electrons, extends the excitation wavelength, and increases the surface-adsorbed amount of dye. We have established that the dispersion of small amounts of GR in TiO_2 can significantly improve the PCE of DSSCs. Optimum concentration (0.09%) of GR in photoanode does not affect the transparency of TiO_2 layer, while significantly increasing the PCE of DSSC, with a maximum value of 4.12%. Thus, we established a profligate, economical, and highly effective technique to enhance the light conversion efficiency of DSSCs.

Acknowledgment

The authors would like to acknowledge the Center of Research Excellence for Renewable Energy, King Fahd University of Petroleum and Minerals, for providing the lab facility.

References

[1] K. W. J. Barnham, M. Mazzer, and B. Clive, "Resolving the energy crisis: Nuclear or photovoltaics?" *Nat. Mater.*, vol. 5, no. 3, pp. 161–164, Mar. 2006.
[2] J.-L. Bredas and J. R. Durrant, "Organic photovoltaics," *Acc. Chem. Res.*, vol. 42, no. 11, pp. 1689–1690, Nov. 2009.
[3] U. Mehmood, S.-ur Rahman, K. Harrabi, I. A. Hussein, and B. V. S. Reddy, "Recent advances in dye sensitized solar cells," *Adv. Mater. Sci. Eng.*, vol. 2014 (Special Issue), p. 12, 2014.
[4] A. Hagfeldt, G. Boschloo, L. Sun, L. Kloo, and H. Pettersson, "Dye-sensitized solar cells," *Chem. Rev.*, vol. 110, no. 11, pp. 6595–6663, Nov. 2010.
[5] N. Robertson, "Optimizing dyes for dye-sensitized solar cells," *Angew. Chem. Int. Ed. English*, vol. 45, no. 15, pp. 2338–2345, May 2006.
[6] C. Klein *et al.*, "Engineering of a novel ruthenium sensitizer and its application in dye-sensitized solar cells for conversion of sunlight into electricity," *Inorg. Chem.*, vol. 44, no. 2, pp. 178–180, Jan. 2005.
[7] M. K. Nazeeruddin *et al.*, "Combined experimental and DFT-TDDFT computational study of photoelectrochemical cell ruthenium sensitizers," *J. Amer. Chem. Soc.*, vol. 127, no. 48, pp. 16835–16847, Dec. 2005.
[8] F. Gao *et al.*, "Enhance the optical absorptivity of nanocrystalline TiO_2 film with high molar extinction coefficient ruthenium sensitizers for high performance dye-sensitized solar cells," *J. Amer. Chem. Soc.*, vol. 130, no. 32, pp. 10720–10728, Aug. 2008.
[9] C.-Y. Chen *et al.*, "Highly efficient light-harvesting ruthenium sensitizer for thin-film dye-sensitized solar cells," *ACS Nano*, vol. 3, no. 10, pp. 3103–3109, Oct. 2009.
[10] A. Kongkanand, R. M. Domínguez, and P. V Kamat, "Single wall carbon nanotube scaffolds for photoelectrochemical solar cells. Capture and transport of photogenerated electrons," *Nano Lett.*, vol. 7, no. 3, pp. 676–680, Mar. 2007.
[11] K. T. Dembele *et al.*, "Graphene below the percolation threshold in TiO_2 for dye-sensitized solar cells," *J. Mater. Chem. A*, vol. 3, no. 6, pp. 2580–2588, Jan. 2015.
[12] U. Mehmood *et al.*, "Hybrid TiO_2–multiwall carbon nanotube (MWCNTs) photoanodes for efficient dye sensitized solar cells (DSSCs)," *Sol. Energy Mater. Sol. Cells*, vol. 140, pp. 174–179, Sep. 2015.
[13] U. Mehmood, S. Ahmed, I. A. Hussein, and K. Harrabi, "Co-sensitization of TiO_2-MWCNTs hybrid anode for efficient dye-sensitized solar cells," *Electrochim. Acta*, vol. 173, pp. 607–612, 2015.
[14] J. Durantini *et al.*, "Photocurrent enhancement in dye-sensitized photovoltaic devices with titania–graphene composite electrodes," *J. Electroanal. Chem.*, vol. 683, pp. 43–46, Sep. 2012.
[15] N. Yang, J. Zhai, D. Wang, Y. Chen, and L. Jiang, "Two-dimensional graphene bridges enhanced photoinduced charge transport in dye-sensitized solar cells," *ACS Nano*, vol. 4, no. 2, pp. 887–894, Feb. 2010.
[16] J. Zhao, J. Wu, M. Zheng, J. Huo, and Y. Tu, "Improving the photovoltaic performance of dye-sensitized solar cell by graphene/titania photoanode," *Electrochim. Acta*, vol. 156, pp. 261–266, Feb. 2015.
[17] U. Mehmood, S. Ahmed, I. A. Hussein, and K. Harrabi, "Improving the efficiency of dye sensitized solar cells by TiO_2–graphene nanocomposite photoanode," *Photon. Nanostructures—Fundam. Appl.*, vol. 16, pp. 34–42, Aug. 2015.

[18] K. I. Bolotin *et al.*, "Ultrahigh electron mobility in suspended graphene," *Solid State Commun.*, vol. 146, nos. 9/10, pp. 351–355, Jun. 2008.
[19] M. D. Stoller, S. Park, Y. Zhu, J. An, and R. S. Ruoff, "Graphene-based ultracapacitors," *Nano Lett.*, vol. 8, no. 10, pp. 3498–3502, Oct. 2008.
[20] Y.-B. Tang *et al.*, "Incorporation of graphenes in nanostructured $TiO_{(2)}$ films via molecular grafting for dye-sensitized solar cell application," *ACS Nano*, vol. 4, no. 6, pp. 3482–3488, Jun. 2010.
[21] S. Sun, L. Gao, and Y. Liu, "Enhanced dye-sensitized solar cell using graphene-TiO_2 photoanode prepared by heterogeneous coagulation," *Appl. Phys. Lett.*, vol. 96, no. 8, p. 083113, Feb. 2010.
[22] U. Mehmood, I. A. Hussein, K. Harrabi, and B. V. S. Reddy, "Density functional theory study on dye-sensitized solar cells using oxadiazole-based dyes," *J. Photon. Energy*, vol. 5, no. 1, p. 053097, Feb. 2015.
[23] U. Mehmood, I. A. Hussein, K. Harrabi, and S. Ahmed, "Density functional theory study on the electronic structures of oxadiazole based dyes as photosensitizer for dye sensitized solar cells," *Adv. Mater. Sci. Eng.*, vol. 2015, p. 8, 2015.
[24] U. Mehmood, I. A. Hussein, M. Daud, S. Ahmed, and K. Harrabi, "Theoretical study of benzene/thiophene based photosensitizers for dye sensitized solar cells (DSSCs)," *Dye Pigment.*, vol. 118, pp. 152–158, Jul. 2015.
[25] H. Mahmood *et al.*, "Band gap reduction of titania thin films using graphene nanosheets," *Mater. Sci. Semicond. Process.*, vol. 24, pp. 193–199, Aug. 2014.
[26] V. Stengl, S. Bakardjieva, T. M. Grygar, J. Bludská, and M. Kormunda, "TiO_2-graphene oxide nanocomposite as advanced photocatalytic materials," *Chem. Cent. J.*, vol. 7, no. 1, p. 41, Jan. 2013.
[27] Y. Zhang, J. Xu, Z. Sun, C. Li, and C. Pan, "Preparation of graphene and TiO2 layer by layer composite with highly photocatalytic efficiency," *Prog. Nat. Sci. Mater. Int.*, vol. 21, no. 6, pp. 467–471, Dec. 2011.
[28] C. H. Tang *et al.*, "Constructing TiO_2/Gr with rapid electrons transfer for efficiency photocatalysis," *Adv. Mater. Res.*, vols. 518–523, pp. 705–708, 2012.
[29] P. Du *et al.*, "Dye-sensitized solar cells based on anatase TiO_2/multi-walled carbon nanotubes composite nanofibers photoanode," *Electrochim. Acta*, vol. 87, pp. 651–656, Jan. 2013.
[30] M.-Q. Yang and Y.-J. Xu, "Basic principles for observing the photosensitizer role of graphene in the graphene–semiconductor composite photocatalyst from a case study on graphene–ZnO," *J. Phys. Chem. C*, vol. 117, no. 42, pp. 21724–21734, Oct. 2013.
[31] Y. Zhang, N. Zhang, Z.-R. Tang, and Y.-J. Xu, "Graphene transforms wide band gap ZnS to a visible light photocatalyst. The new role of graphene as a macromolecular photosensitizer," *ACS Nano*, vol. 6, no. 11, pp. 9777–9789, Nov. 2012.
[32] L. Han *et al.*, "Improvement of efficiency of dye-sensitized solar cells by reduction of internal resistance," *Appl. Phys. Lett.*, vol. 86, no. 21, p. 213501, May 2005.
[33] G. C. Q. Zhang, T. P. Chou, B. Russo, and S. A. Jenekhe, "Polydisperse aggregates of ZnO nanocrystallites: A method for energy-conversion-efficiency enhancement in dye-sensitized solar cells," *Adv. Funct. Mater.*, vol. 18, pp. 1654–1660, 2008.
[34] K. Lee, C. Hu, H. Chen, and K. Ho, "Incorporating carbon nanotube in a low-temperature fabrication process for dye-sensitized TiO_2 solar cells," *Sol. Energy Mater. Sol. Cells*, vol. 92, no. 12, pp. 1628–1633, Dec. 2008.
[35] Y.-L. Xie, Z.-X. Li, Z.-G. Xu, and H.-L. Zhang, "Preparation of coaxial TiO_2/ZnO nanotube arrays for high-efficiency photo-energy conversion applications," *Electrochem. Commun.*, vol. 13, no. 8, pp. 788–791, Aug. 2011.
[36] S. Li *et al.*, "Preparation and performance of dye-sensitized solar cells based on ZnO-modified TiO_2 electrodes," *Int. J. Miner. Metall. Mater.*, vol. 17, no. 1, pp. 92–97, Feb. 2010.
[37] K. T. Dembele *et al.*, "Hybrid carbon nanotubes–TiO_2 photoanodes for high efficiency dye-sensitized solar cells," *J. Phys. Chem. C*, vol. 117, no. 28, pp. 14510–14517, Jul. 2013.

Authors' photographs and biographies not available at the time of publication.